JOURNAL OF GEOPHYSICAL RESEARCH, VOL. 108, NO. D15, 4438, doi:10.1029/2003JD003537, 2003

Synthesis inverse mapping method applied to the retrieval of aerosol size distributions from extinction measurements

Didier Fussen, Filip Vanhellemont, and Christine Bingen
Institut d'Aéronomie Spatiale de Belgique, Brussels, Belgium

Received 26 February 2003; revised 24 April 2003; accepted 9 May 2003; published 2 August 2003.

[1] The problem of inverting aerosol extinction data in the near-UV to near-IR range to retrieve aerosol size distributions is addressed by means of a recently developed method called "synthesis inverse mapping." The rationale and the algebra of the method are developed, and the full error budget is discussed. The performance of the algorithm is evaluated with respect to standard monomodal and bimodal distributions published in the literature. The new method allows error amplification control and estimation of the smoothing error, and it is well suited for operational fast retrieval. *INDEX TERMS:* 0305 Atmospheric Composition and Structure: Aerosols and particles (0345, 4801); 4801 Oceanography: Biological and Chemical: Aerosols (0305); *KEYWORDS:* inversion, aerosol size distribution, extinction coefficient

Citation: Fussen, D., F. Vanhellemont, and C. Bingen, Synthesis inverse mapping method applied to the retrieval of aerosol size distributions from extinction measurements, *J. Geophys. Res.*, *108*(D15), 4438, doi:10.1029/2003JD003537, 2003.

1. Introduction

[2] Remote sounding of stratospheric aerosols from spaceborne optical experiments in the near-UV to near-IR range leads unavoidably to a difficult inverse problem. In limb occultation geometries, the atmospheric transmittance along the optical path between the light source (a star, a planet, the Sun or the Moon) and the detector can usually be measured with a good precision over an extended spectral domain. Besides the necessity of retrieving the local optical thickness of each atmospheric layer by carrying out a vertical inversion of the measured slant path transmittance, it is also necessary to perform a spectral inversion to separate the contributions of different absorbing (or scattering) constituents. Most atmospheric gases attenuate the incoming light at different wavelengths according to their extinction cross section, a quantity measurable in the laboratory, which allows the retrieval of the gas number density. However, the wavelength dependence of the aerosol extinction, albeit smooth, is a priori unknown and it is actually a product of the spectral inversion. Consequently, it is virtually impossible to retrieve the exact analytical shape of the aerosol extinction if it competes with absorbing gases having a smooth cross section in the same spectral domain [*Fussen et al.*, 2002a]. For a given signal-to-noise ratio a trade-off has to be sought between systematic and random retrieval errors and, in realistic circumstances, the composite total error can hardly be reduced below a 10% level.

[3] Assuming a minimal knowledge of the stratospheric aerosol composition, it is possible to derive supplementary information about the aerosol particle size distribution by describing the retrieved aerosol extinction coefficient within the frame of Mie scattering theory. This is the context of an optical inversion problem which is a notoriously ill-posed problem due to the large dynamic range in which the particle distribution has to be retrieved and also because of the unbounded nature of the Mie cross section.

[4] In the past, many authors have addressed this question. In order to avoid a fastidious enumeration, we refer the reader to the extensive review of existing approaches given by *Steele and Turco* [1997] and *Yue* [1999]. Briefly, one could summarize the difficulty of the optical inversion as follows: the aerosol extinction coefficient results from the integration, hence the smoothing, of the extinction cross section weighted by the relative population of particle classes. The fundamental nature of the problem lies in the amplification of high frequencies observed in the signal. Therefore any experimental noise added to the true signal will cause very large unphysical (i.e., not related to the true unknown aerosol distribution) spurious oscillations in the solution. Although this behavior is not suspect, it prevents retrieved data to be trusted by possible users and it is aesthetically or philosophically frustrating, a psychological factor that cannot be underestimated in the quest for an "ideal" inversion scheme. Basically, almost all proposed methods rely on the adjunction of supplementary (and/or arbitrary) information in order to regularize the ill-posed problem [*Rodgers*, 2000]. The incorporation of auxiliary information can be performed on the basis of Bayesian methods leading to the so-called optimal estimation methods or by pure regularization techniques like Twomey-Tikhonov constrained linear inversions. Also, regularization can be achieved by using constrained fitting with respect to preselected analytical shapes of the aerosol particle size distribution.

[5] In a recent publication [*Fussen et al.*, 2002b], we presented a new robust inversion technique that could be applied to inverse problems in geophysics. This method is

0148-0227/03/2003JD003537

called "synthesis inverse mapping" (SIM) because it tries to apprehend the difficulties associated with the algebraic or iterative inversion. Instead, it makes use of a synthetic construction of an inversion operator that is capable to map the measurement space onto the space of "acceptable" solutions.

[6] In this article, we will present how the SIM method can be applied to the retrieval of aerosol particle size distributions from their extinction coefficient measured from the UV to the near IR range. Our intention is more to underline the advantages of the SIM technique as well to confirm the intrinsic limitations of the optical inversion already mentioned by other authors. Also, it is very difficult to perform an extensive benchmark of already proposed methods. Therefore we decided to apply the method to the six typical lognormal cases proposed by *Steele and Turco* [1997] (referred to as "SLN" hereafter) and to show that the method possesses the following qualities: robustness, operational simplicity, positivity of the solution and assessment of the full error budget. The proposed method can be applied to limb occultation measurements but is also useful for the ground-based Sun photometry [*Dubovik and King*, 2000; *Schmid et al.*, 1997; *King et al.*, 1978].

2. Statement of the Problem

[7] Hereafter, we will consider optical measurements of the aerosol extinction coefficient for wavelengths λ ranging from $\lambda_1 = 0.2$ μm, certainly a lower limit for stratospheric transmittance, to $\lambda_2 = 1.6$ μm where informative content of the measurement gets progressively dominated by aerosol composition rather than by the geometrical characteristics of the scattering particles (the SAGE III experiment recently launched in December 2001 has an outermost aerosol channel at 1.55 μm). Also, we will consider a continuous variation of λ because modern instrumentation makes use of 1 nm spectral resolution or better. Clearly however, 1000 pixels do not mean 1000 pieces of independent information in the retrieved extinction spectrum because the experimental or retrieval noise obscures the little information content of adjacent pixels when their redundancy is removed out. The extinction coefficient $\beta(\lambda)$ for a population of aerosol droplets of radius r characterized by a Mie extinction efficiency $Q(r, \lambda)$ may be written as:

$$\beta(\lambda) = \int_0^{\infty} C(r,\lambda) f(r)\, dr \simeq \int_0^{r_m} C(r,\lambda) f(r)\, dr = \int_0^{r_m} \pi r^2 Q(r,\lambda) f(r)\, dr, \quad (1)$$

where the considered domain for the particle size is reduced to $r_m = 1$ μm, a value for which the typical sedimentation velocity is about 2 km/year at 25 km, preventing the observation of such big particles in normal volcanic periods. This upper limit for r could be increased in the aftermath of a major eruption if the instrument is not in saturation mode due to the excessive slant path optical thickness. In equation (1), $C(r, \lambda)$ stands for the usual Mie extinction cross section computed by assuming a standard composition of 25% H_2O and 75% H_2SO_4 by weight (refractive index = 1.43). The optical inversion problem can now be formulated by: "What is the particle size distribution $f(r)$ that produced the retrieved $\beta(\lambda)$?"

[8] Owing to the intrinsic microphysical evolution of the aerosol particles in coagulation and condensation/evaporation processes, the estimated value of $f(r)$ makes sense over several orders of magnitude and is usually represented on a logarithmic scale. This is enhanced by the quadratic variation of $C(r, \lambda)$ with increasing r values. Instead of rescaling $f(r)$ by using a generic $f_0(r)$ function (e.g., a Junge-type weighting function as used by *Steele and Turco* [1997]), we directly write:

$$f(r) = \exp(a_0 + a_1 U_1(r) + \ldots a_{n_r} U_{n_r}(r)), \quad (2)$$

where $U_i(r)$ is the Chebyshev polynomial of the first kind of order i defined by:

$$U_i(r) = \cos\left(i \cos^{-1}\left(\frac{2r - r_m}{r_m}\right)\right). \quad (3)$$

[9] Besides its natural ability to describe large variations of $f(r)$, the expansion of the exponential argument in equation (2) constrains the final solution to be always positive which meets the physical intuition. Furthermore, the use of a basis of orthogonal polynomials allows a degressive description of the unknown function as the polynomial order is increased. The choice of Chebyshev polynomials is not essential; over a finite interval, they are known to approximate the minimax polynomial. However, another family of orthogonal polynomials (e.g., Legendre) could be successfully used. Hereafter, we will mostly use $n_r = 5$, for two reasons. First, our objective is to test the SIM method on cases (see Table 1) where the particle size distribution can be bimodal and hence susceptible to be described by 6 independent parameters. Second, the signal-to-noise ratios usually met in remote sounding experiments do not allow to retrieve much more than 4 to 6 aerosol parameters over the considered wavelength range (we refer the reader to the excellent and still up-to-date book of *Twomey* [1985] for a general discussion of the information content carried by $\beta(\lambda)$). It is clear that the inversion problem will now result in the determination of some vector of unknown coefficients $\vec{a}^{\mathrm{T}} = (a_0 a_1 \ldots a_{nr})$; notice that the nonlinear dependence of the solution on $\vec{a}$ has to be kept in mind when performing a computation of error propagation.

[10] In a similar way as the linear minimizing error (LME) approach proposed by *Yue* [1999], the SIM method needs a subspace of possible solutions for the mapping. However, unlike LME, no particular assumption is made on the analytical shape of the solution as a lognormal distribution or as a sum of two lognormals in order to describe bimodality. The expansion in equation (2) is sufficiently general to describe any distribution if n_r is large enough or to describe the most general distribution having $(n_r + 1)$ degrees of freedom. An easy way to construct a subspace of K possible solutions is to randomly generate K ensembles of (n_r+1) points on the $[0,r_m]$ interval and to compute the corresponding $\vec{a}^{[k]}$ $\{k = 1 \ldots K\}$ of the collocating Chebyshev expansions. Also, we allow the drawing to be rejected if any point of the associated $f^{[k]}(r)$ does not lie in a given band of considered possible values. A reasonable value of K is $3^{(n_r+1)}$ (= 729 for $n_r = 5$) as it would be

Table 1. Six Test Cases Selected by *Steele and Turco* [1997][a]

Case	Type	N_1, cm^{-3}	ρ_1, μm	σ_1	N_2, cm^{-3}	ρ_2, μm	σ_2
A	monomodal	10.0	0.0725	1.86	–	–	–
B	monomodal	0.96	0.0900	1.80	–	–	–
C	bimodal	6.00	0.1100	1.67	3.40	0.4300	1.36
D	bimodal	2.61	0.1100	1.43	1.84	0.3000	1.48
E	bimodal	1.25	0.1300	1.58	1.28	0.5600	1.26
F	bimodal	1.29	0.0900	1.41	1.69	0.3900	1.30

[a]The particle size distribution $f(r)$ reads: $f(r) = \Sigma_{i=1}^{2} \frac{N_i}{\sqrt{2\pi} r \ln(\sigma_i)} \cdot \exp(-\frac{\ln^2(\frac{r}{\rho_i})}{2\ln^2(\sigma_i)})$.

obtained by all combinations of each a_i coefficient taking a low, a median and a high value. In Figure 1, we present the domain of possible solution subspace and the associated set of extinction coefficients. The SLN test distributions are also shown. Notice that the inversion method will be able, by construction, to detect that a solution is suspicious when it falls outside the generated solution subspace which should then be enlarged.

[11] We will perform a quite symmetrical description of the retrieved extinction coefficient, the range of which may also span several decades. First, we introduce a rescaling operation as:

$$g(\lambda) = \sinh^{-1}(\kappa\beta(\lambda)), \tag{4}$$

where the value of κ can be set to 10^4 or larger. The function $\sinh^{-1}(x)$ has the interesting properties of a linear variation for small absolute values of the argument and logarithmic behavior for large values, i.e.,

$$\sinh^{-1}(x) = \ln(x + \sqrt{1+x^2}) = -\sinh^{-1}(-x) \tag{5}$$

$$\approx x \qquad |x| \ll 1 \tag{6}$$

$$\approx \ln(2x) \qquad x \gg 1, \tag{7}$$

and the exponential-like histogram of $\beta^{[k]}(\lambda)$ values is now transformed into a more balanced distribution (see Figure 2). Also, the possible occurrence of negative β's due to added experimental noise will not cause particular problems which would not be the case if we had simply used a logarithmic transformation instead of equation (4). Second, we describe the transformed extinction spectrum by a similar Chebyshev expansion as:

$$g(\lambda) = (b_0 + b_1 V_1(\lambda) + \ldots b_{n_\lambda} V_{n_\lambda}(\lambda)), \tag{8}$$

where n_λ is greater or equal to n_r to avoid underdetermination of the problem (for $n_r = 5$, an accurate description of $g(\lambda)$ could be achieved for $n\lambda = 10$). The Chebyshev polynomials $V_j(\lambda)$ are now defined by:

$$V_j(\lambda) = \cos\left(j \cos^{-1}\left(\frac{2\lambda - (\lambda_1 + \lambda_2)}{\lambda_2 - \lambda_1}\right)\right). \tag{9}$$

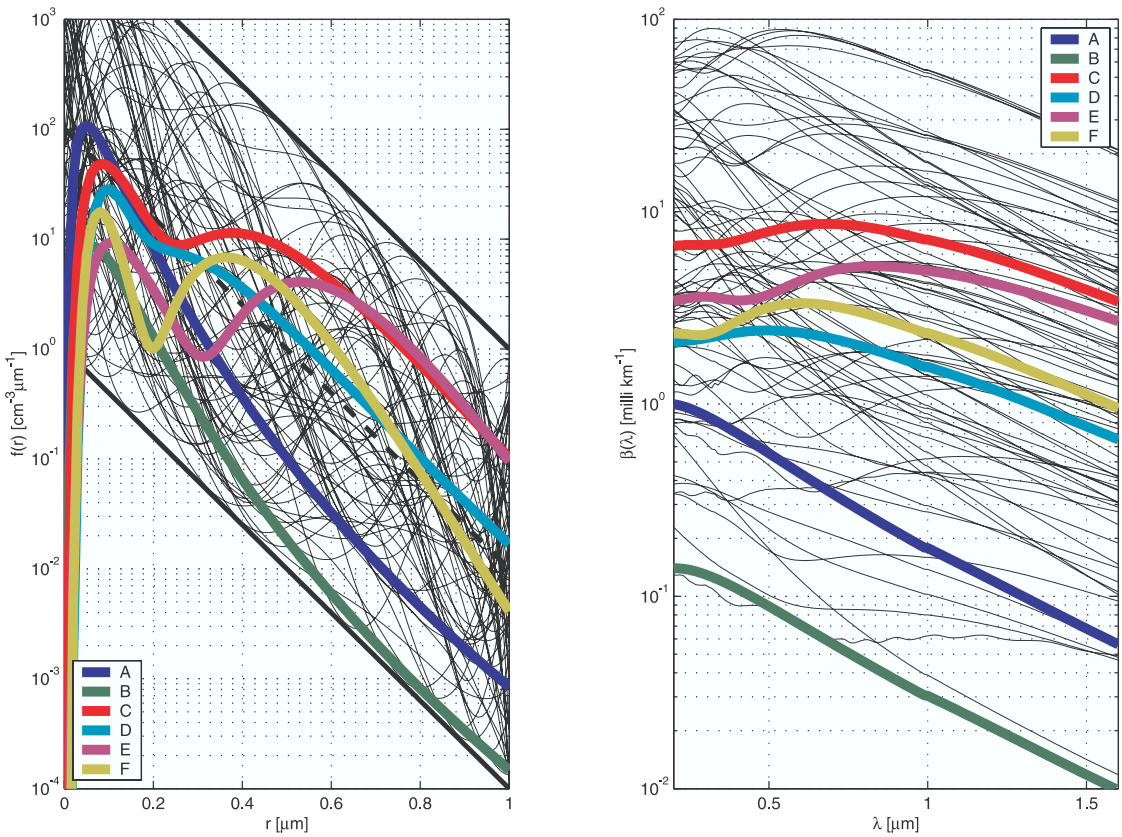

Figure 1. (left) Thin black lines, ensemble of possible solutions (decimated for the sake of readability); thick black lines, upper and lower solution bounds; dashed black line, median solution; colored lines, the 6 test cases of Table 1). (right) Corresponding extinction spectra.

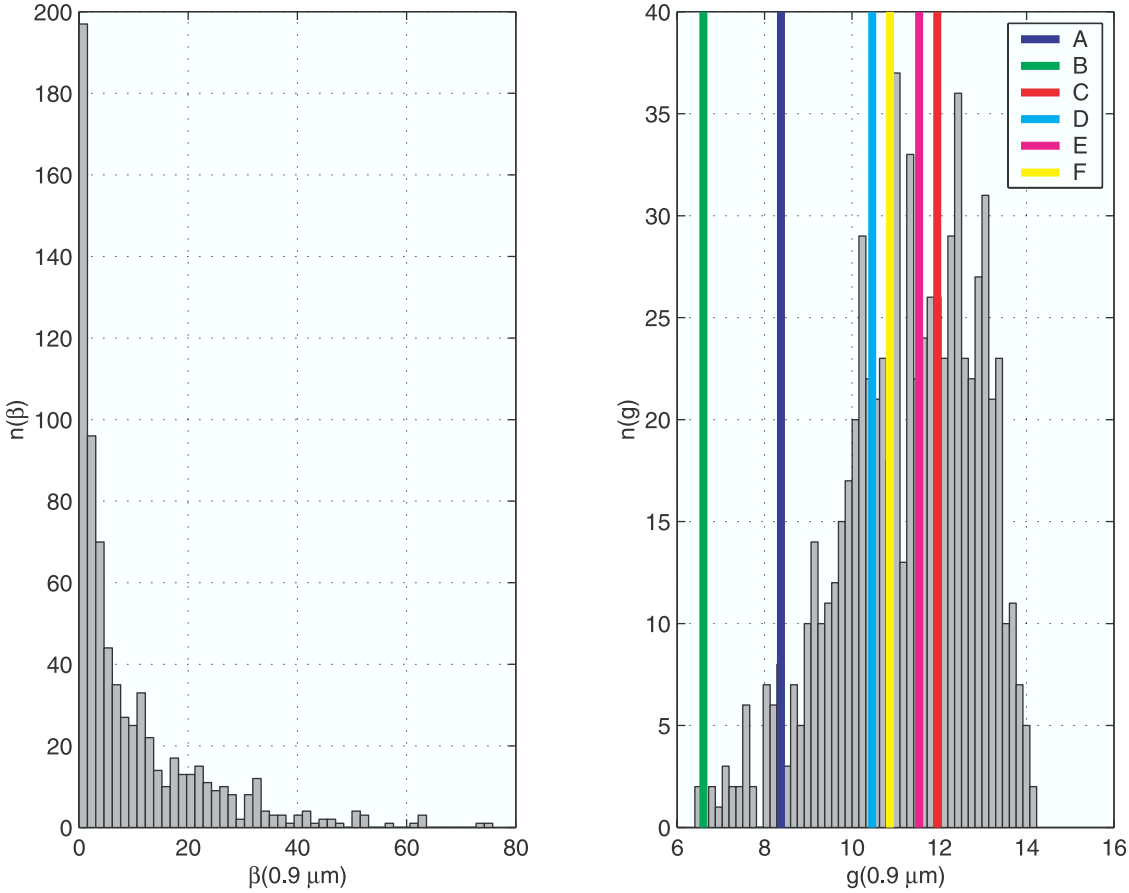

Figure 2. (left) Histogram of extinctions at $\lambda = 0.9$ μm generated from the ensemble of possible solutions. (right) Histogram of transformed extinctions $g(\lambda)$ (see equation (4)); the colored lines indicate the position of the values of the six test cases reported in Table 1.

[12] The basic idea of the SIM method consists in the construction (hence the name "synthesis") of an inversion operator B capable of mapping all the b_j coefficients onto the a_i set. Summarizing the theoretical arguments developed by *Fussen et al.* [2002b], B should be accurate enough to describe any solution contained in the possible solution subspace but B is constrained to suppress high-frequency noise amplification in the same range. Notice that a quite natural noise filtering is already performed in equation (8) where the first b_j's capture mainly low-frequency information.

[13] In the most simple form (referred to as SIM1), we will first consider a linear dependence on the b_j's and, for each coefficient a_i, we may write:

$$\begin{pmatrix} \delta b_0^{[1]} & \delta b_1^{[1]} & \cdots & \delta b_{n_\lambda}^{[1]} \\ \delta b_0^{[2]} & \delta b_1^{[2]} & \cdots & \delta b_{n_\lambda}^{[2]} \\ \vdots & \vdots & \ddots & \vdots \\ \delta b_0^{[K]} & \delta b_1^{[K]} & \cdots & \delta b_{n_\lambda}^{[K]} \end{pmatrix} \begin{pmatrix} B_{i0} \\ B_{i1} \\ \vdots \\ B_{in_\lambda} \end{pmatrix} = \begin{pmatrix} \delta a_i^{[1]} \\ \delta a_i^{[2]} \\ \vdots \\ \delta a_i^{[K]} \end{pmatrix} \tag{10}$$

for which $\delta a_i^{[k]} = a_i^{[k]} - \overline{a_i}$ and $\delta b_j^{[k]} = b_j^{[k]} - \overline{b_i}$ where $\overline{a_i}$ and $\overline{b_i}$ respectively stand for the mean values of $a_i^{[k]}$ and $b_j^{[k]}$ averaged over the K simulations represented by the rows of the matrix. Equation (10) is more conveniently expressed by

$$D\,\vec{B}_i = \overrightarrow{\delta A}_i. \tag{11}$$

[14] The least squares solution of equation (11) is easily calculated as

$$\vec{B}_i^{LS} = (D^T D)^{-1} D^T \overrightarrow{\delta A}_i, \tag{12}$$

which is naturally unstable due to the lowest eigenvalues of the covariance matrix $D^T D$, i.e., the elements of $\vec{B}_i^{LS}$ tend to be very large and they will overamplify any experimental noise added to the δb_j in the left-hand side of equation (11). On the other hand, we know from our simulation of the K forward model realizations that the solution to the inversion of the $\overrightarrow{\delta A}_i$ must lie in the δa_i distributions, hence it is certainly reasonable to impose that the variance of the retrieved solutions should equal the initial ensemble variance by applying a constraint on the size of the $\vec{B}_i$ elements:

$$\vec{B}_i^T\,\overline{\Delta b^2}\,\vec{B}_i = \vec{B}_i^T \begin{pmatrix} \overline{\delta b_0^2} & 0 & \cdots & 0 \\ 0 & \overline{\delta b_1^2} & \cdots & 0 \\ \vdots & \vdots & \ddots & \vdots \\ 0 & 0 & \cdots & \overline{\delta b_{n_\lambda}^2} \end{pmatrix} \vec{B}_i = \overline{\delta a_i^2}, \tag{13}$$

where the $\overline{\delta b_i^2}$ elements stand for the respective variances of the δb_i associated with the K simulations.

[15] The determination of the inversion operator reduces now to the constrained minimization of a merit function L_i that combines two criteria: closeness to simulated data and

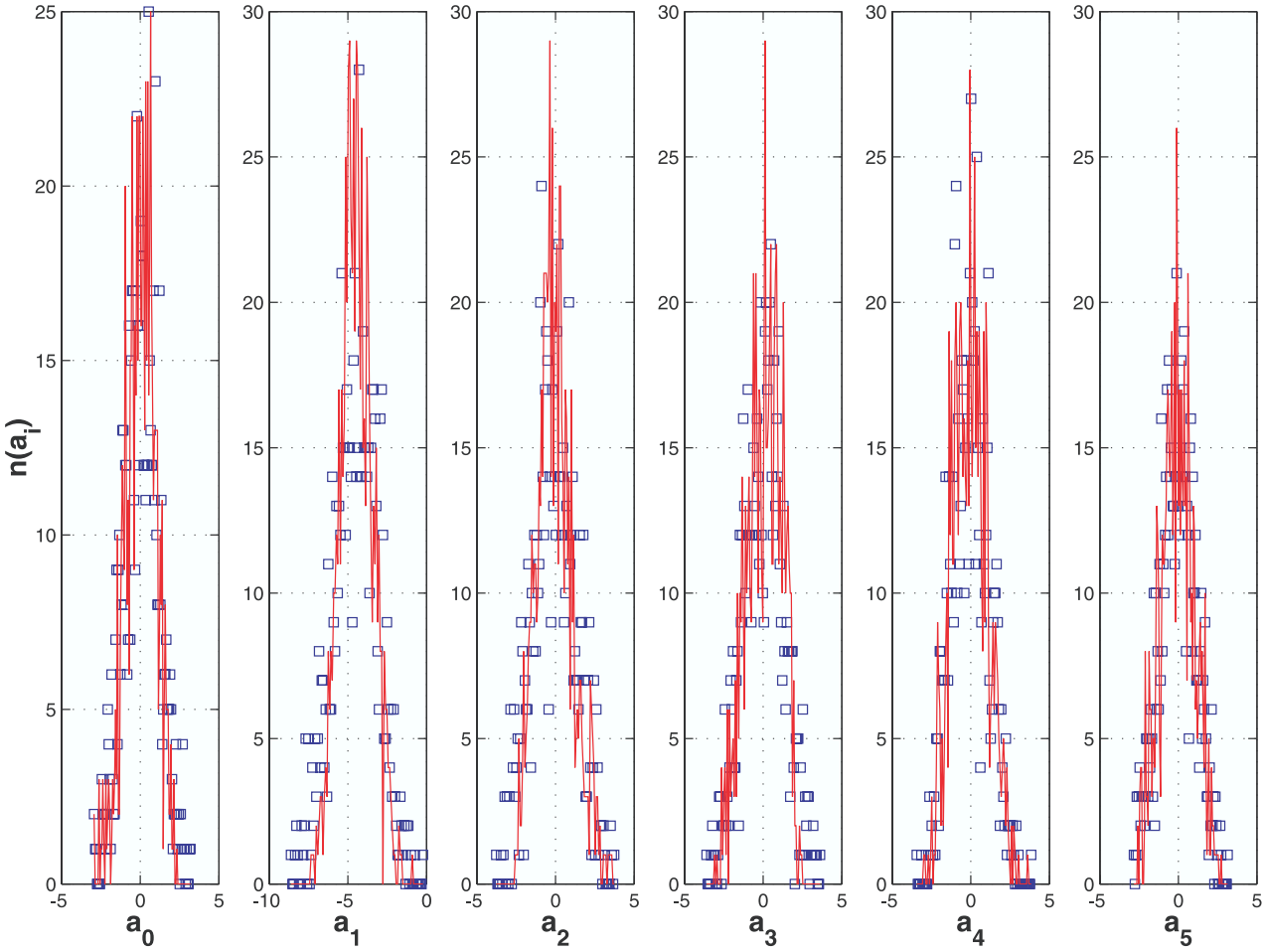

Figure 3. Histograms (100 bins) of a_i coefficients for n_r = 5. Squares, possible solution set. Red line, retrieved distribution of a_i^R for SIM3.

regularization compatible with the selected variability of the synthetic (and noiseless) simulations. L_i reads:

$$L_i = ||D\vec{B}_i - \overrightarrow{\delta A}_i||^2 + \theta_i\left(\vec{B}_i^T\overline{\Delta b^2}\vec{B}_i - \overline{\delta a_i^2}\right), \quad (14)$$

where θ_i is the Lagrange multiplier. Formally, the last equation looks similar to various constrained linear inversion methods. Here, however, the Lagrange multiplier θ_i is not a "trade-off" parameter that can be arbitrarily tuned but it really constrains the solution not to extend outside the bounds that have been used for simulating the mapping between both solution and measurement domains. In other words, there is only one solution for θ_i and this value represents a hard constraint (equation (13)). The value of $\vec{B}_i^*$ that minimizes L_i can be algebraically obtained as:

$$\vec{B}_i^* = \vec{B}_i^*(\theta_i) = (D^TD + \theta_i\overline{\Delta b^2})^{-1}D^T\overrightarrow{\delta A}_i, \quad (15)$$

whereas the value of θ_i can be found by numerically solving the secular equation [*Golub and Van Loan*, 1996]:

$$\vec{B}_i^{T*}(\theta_i)\,\overline{\Delta b^2}\,\vec{B}_i^*(\theta_i) - \overline{\delta a_i^2} = 0. \quad (16)$$

[16] The complete construction of B requires n_r + 1 resolutions of equations (15) and (16) but this has to be performed only once. It is also clear that any signal that will belong to the subspace spanned by the synthetic extinction set will produce a reasonable solution inside the possible solution domain spanned by the K simulations.

[17] If we want a more accurate inversion, it is also possible to generalize SIM1 to a nonlinear dependence on the δb_j if the number of coefficients to compute is not underdetermined with respect to K. For instance, a third-order expansion (SIM3) can be written as:

$$\delta a_i = \sum_{j=0}^{n_\lambda} B_{ij}\delta b_j + \sum_{j=0}^{n_\lambda}\sum_{k=j}^{n_\lambda} B_{ijk}\delta b_j\delta b_k + \sum_{j=0}^{n_\lambda}\sum_{k=j}^{n_\lambda}\sum_{l=k}^{n_\lambda} B_{ijkl}\delta b_j\delta b_k\delta b_l, \quad (17)$$

where the $B_{ij.l}$ can be computed in the same way as described by equations (14 to 16). The number of coefficients to compute increases however exponentially with the SIM order (11 for SIM1, 77 for SIM2, 363 for SIM3 if we use n_λ = 10 in the signal analysis).

3. Application of the SIM Method and Error Budget

[18] In Figure 3, we have plotted the histograms of the a_i set of the 729 synthetic possible solutions and also, by

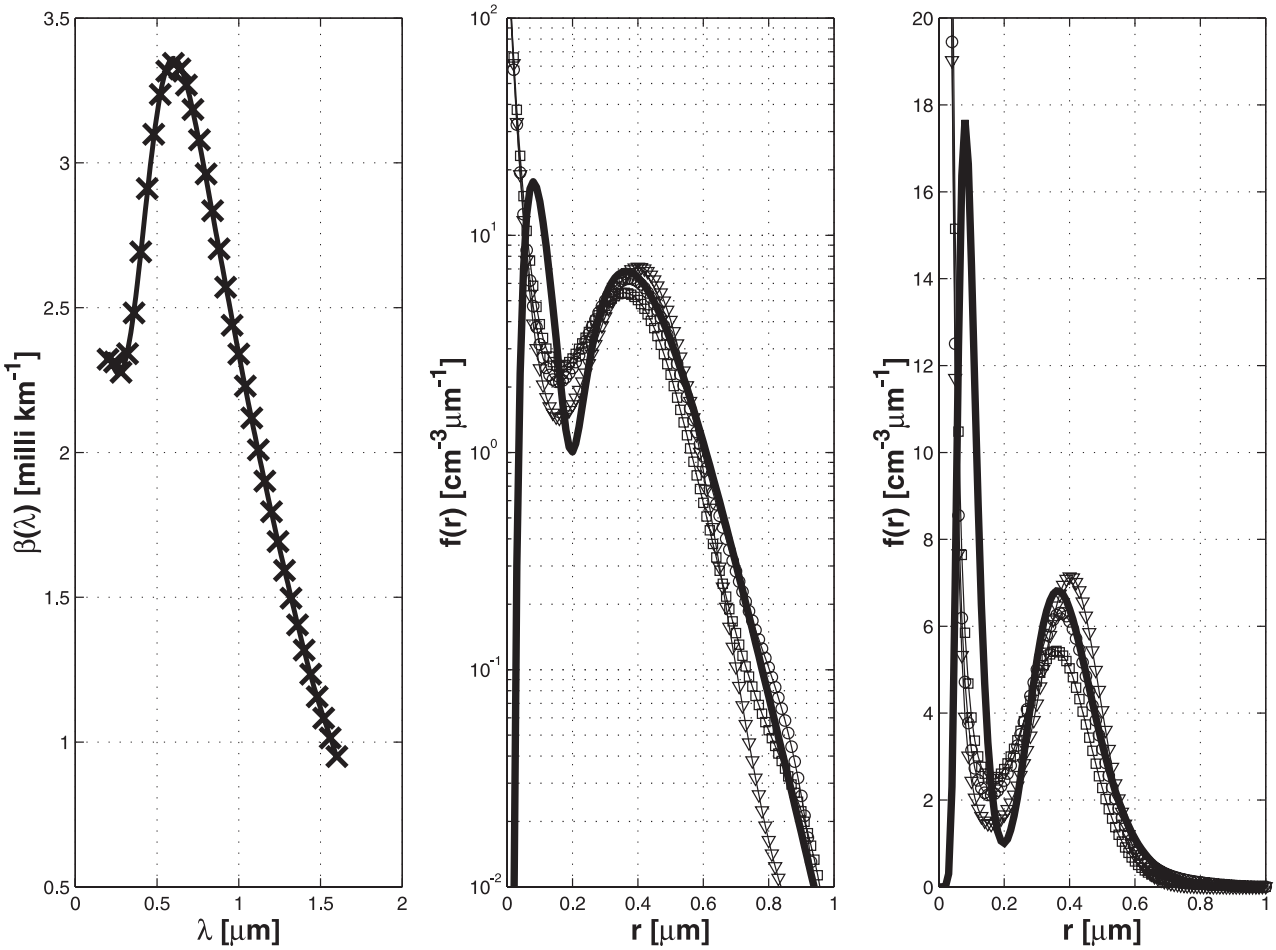

Figure 4. (left) Extinction coefficient for the test case F; crosses, signal values (only 1 point over 4 plotted for readibility); full line, Chebyshev expansion for n_λ = 10. (middle) Full line, the exact distribution for test case F; triangles, SIM1; squares, SIM2; circles, SIM3. (right) Same as central plot for a linear scale.

application of equation (11), the retrieved a_i^R distribution for the SIM3 computation. Clearly, the a_i^R values are well confined within the simulation values, which means that any noisy signal that can be developed according to equation (8) with coefficients b_j belonging to the simulated distribution will produce a solution within the possible solution subspace. This means that singular or unrealistic measurements can be flagged before the inversion by checking that their b_j distributions lie outside the expected values. In such a case, the measurement should be rejected as corrupted by a possible low-frequency perturbation, virtually indistinguishable from the true signal. If many measurements are flagged, it means that the atmospheric state is very unusual and that the possible solution ensemble has to be enlarged.

[19] In Figure 4, we present the aerosol extinction signal produced by the F test case distribution and the results of the SIM inversion, for different orders. Although the improvement is not spectacular, there is a clear evidence that the SIM3 computation is the most accurate. The large extreme in the $\beta(\lambda)$ curve is clearly caused by the corresponding large particle lobe in the particle size distribution confirming the intuitive idea that particles of a given characteristic size diffract efficiently incident light at roughly the same wavelength value. The large particle mode is reasonably well retrieved over a large dynamical scale. However, for the same reason, it is also clear that the distribution retrieval is much poorer below 0.2 μm. As pointed out by *Steele and Turco* [1997] and *Thomason* [1991], there is very little information about small aerosol particles due to the quadratic weighting by $C(r, \lambda)$ in equation (1). This suggests that the small particle mode is virtually impossible to detect when other modes of larger particles coexist.

[20] In Figures 5 and 6, respectively on logarithmic and linear scales, we present the results of the SIM3 inversion for the six test cases (see parameters in Table 1). Taking into account the above mentioned remarks, the general agreement is acceptable, in particular for pure monomodal (distributions A and B) and pure bimodal cases (E and F). The agreement is less satisfactory for cases C and D because there is an overlap of both modes that weakens their respective spectral signatures in $\beta(\lambda)$.

[21] Comparing the relative efficiency of different optical inversion methods is a tedious and difficult task that will be addressed in further work. For instance, *Yue* [1999] does not

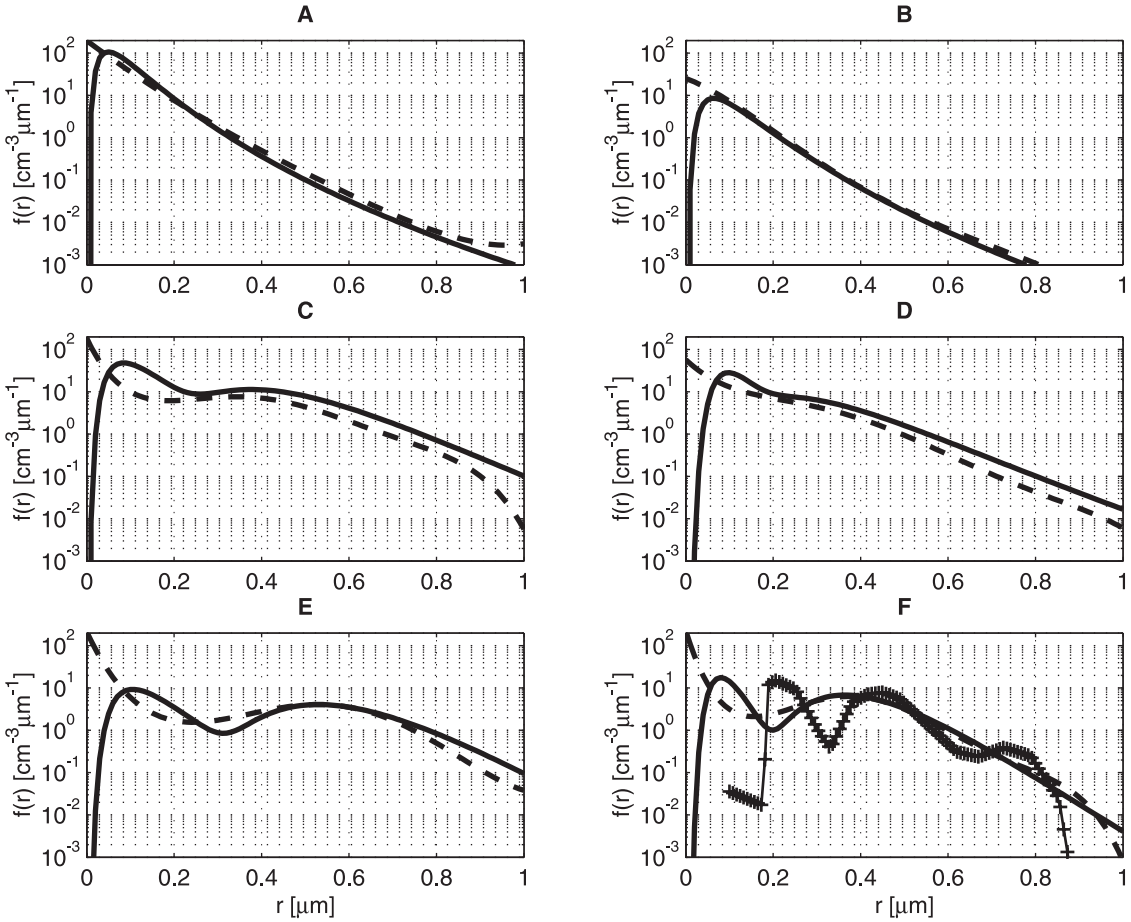

Figure 5. Comparison, on logarithmic scale, of SIM3 retrieved distributions (dashed lines) and test cases (full lines). For the test case F we also report the CLI result obtained by *Steele and Turco* [1997], which is clearly less stable than the SIM distribution.

tabulate the coefficients of his LME method for the retrieval of the particle size distribution (only the coefficients for the aerosol surface area and volume densities are given) and he does not give a quantitative criterion (''..a reasonable number of new sets..'') to stop the iteration in the computation of the coefficient set. Also, it is not clear how he can retrieve the particle size distribution in 18 bins from only 4 SAGE II extinction channels which implies that an important redundancy exists between the retrieved bins. A rigorous comparison between different methods should be done for a number of parameters or bins compatible with the information content of the measurement, at most 4 in that case. This underdetermination problem is also present in the CLI method studied by *Steele and Turco* [1997] where 30 bins are used that make the inversion ill-posed. Consequently, the selection of a single solution relies on a priori knowledge and intuition, a rather inefficient technique for operational processing of large extinction data sets. Indeed, the redundancy between the bins is responsible for the small eigenvalues that cause instability of the retrieved distribution as clearly demonstrated by *Twomey* [1985]. This instability cannot always be attenuated by using a large Lagrange multiplier. In Figures 5 and 6, we report the bimodal case F as inverted by using the CLI method. It is interesting to point out that the result does not improve when 11 channels were used instead of 4. Here also, the present SIM method seems to be more robust by nature.

[22] The efficiency of the SIM method to restrain excessive noise amplification has been illustrated in Figure 7. It is always possible to compute the usual least squares solution by setting $\theta_i = 0$ in equation (15). Although it provides an accurate inversion formula (actually, somewhat more accurate than the SIM3 solution), this solution is intrinsically unstable due to the very low eigenvalues in the design matrix spectrum. As a consequence, the noise is overamplified by the inversion process. On the contrary, the SIM3 inversion will constrain the noisy solution to stay in the possible solution subspace.

[23] Synthetic methods also possess a fundamental advantage: apart from allowing the estimation of the random error amplification, they naturally produce an estimation of the smoothing (or systematic) error of the inversion. The smoothing error can be defined as the error resulting from the combined application of the forward model-retrieval process. Ideally, this should give a unit matrix but this is not the case due to the ill-posedness of the problem. As quoted by *Rodgers* [2000], there is a priori no way to know the smoothing error because the exact solution used to compute it is unknown. However, a good estimation can be per-

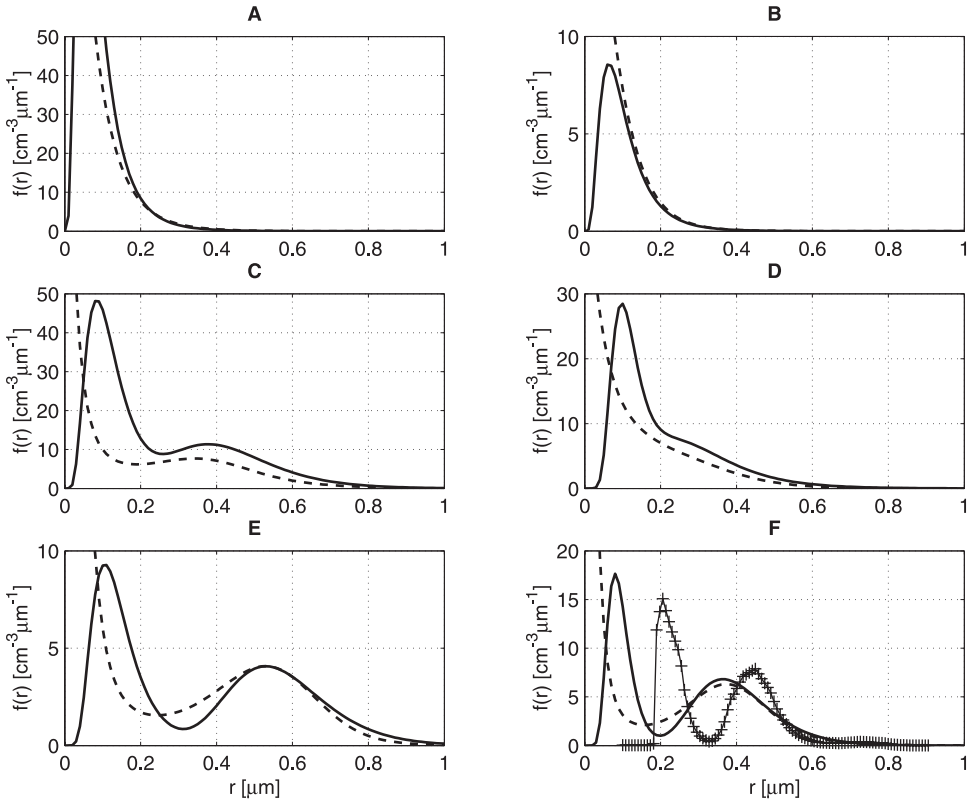

Figure 6. Same as in Figure 5, but on a linear scale.

formed if we use a subspace of synthetic examples to which the true particle size distribution is expected to belong. Standard first-order error propagation applied to equation (2) leads to:

$$\Delta f(r) \simeq \frac{\partial f}{\partial a_0}\Delta a_0 + \frac{\partial f}{\partial a_1}\Delta a_1 + \ldots + \frac{\partial f}{\partial a_{n_r}}\Delta a_{n_r} = \overrightarrow{\Delta a}^{\mathrm{T}}\overrightarrow{U(r)}\, f(r), \tag{18}$$

($\overrightarrow{U(r)}$ is the array of (n_r + 1) Chebyshev polynomials) and the smoothing error covariance matrix $S_s(r)$ of the retrieved distribution can be estimated by

$$S_s(r) = f(r)^2 \overrightarrow{U}^T S_a \overrightarrow{U}. \tag{19}$$

[24] In the latter expression, S_a the error covariance matrix on the retrieved a_i coefficients is evaluated as:

$$S_a = \frac{1}{K}\sum_{k=1}^{K}\left(\overrightarrow{a^{[k]}}^{\mathrm{R}} - \overrightarrow{a^{[k]}}\right)^T\left(\overrightarrow{a^{[k]}}^{\mathrm{R}} - \overrightarrow{a^{[k]}}\right), \tag{20}$$

whereas the random error covariance S_r can be computed on the same way from the experimental error covariance matrix $S\beta$ propagating through equations (4) and (15).

[25] In Figure 8, we present the error budget for a 5% Gaussian noise added to the experimental extinction curve produced by the median distribution of the possible solution subspace. Clearly, the standard least squares solution ($\theta_i = 0$) provides a more accurate resti tution of the median distribution with a minimal error of about 3% at $r_0 \simeq 0.4$ µm whereas the minimal error produced by SIM3 is about 30% in the same domain. However, this advantage of the LS inversion is completely obscured by the catastrophic random error amplification up to about 3000% while this is not the case for the SIM3 inversion. Consequently, the experimental error level should be lowered by a factor 100 before preferring the least squares inversion, an unrealistic requirement in a remote sensing experiment.

4. Conclusions

[26] The synthesis inverse mapping (SIM) method has been successfully applied to the difficult problem of the aerosol extinction coefficient inversion. With respect to most of the proposed approaches found in the literature, SIM proposes interesting alternatives. First, the method deals with the mapping of low-frequency components between the signal and solution spaces by using limited expansion in terms of orthogonal polynomials, recognizing that spurious structures produced in the retrieved distributions arise from overamplification of high-frequency components, mainly noise. Second, the SIM scheme focuses on the amplification control by constraining the inversion of noisy data to lie in the possible solution subspace if the signal expansion over the polynomial basis belongs to the subspace of possible extinctions. If it is not the case, the measurement may be rejected with confidence or the possibility of a very unusual atmospheric aerosol has to be considered. Third, the SIM method allows to assess a full error budget of the inversion algorithm and consequently it may be used to optimize the accuracy of the inversion until it reaches a predetermined

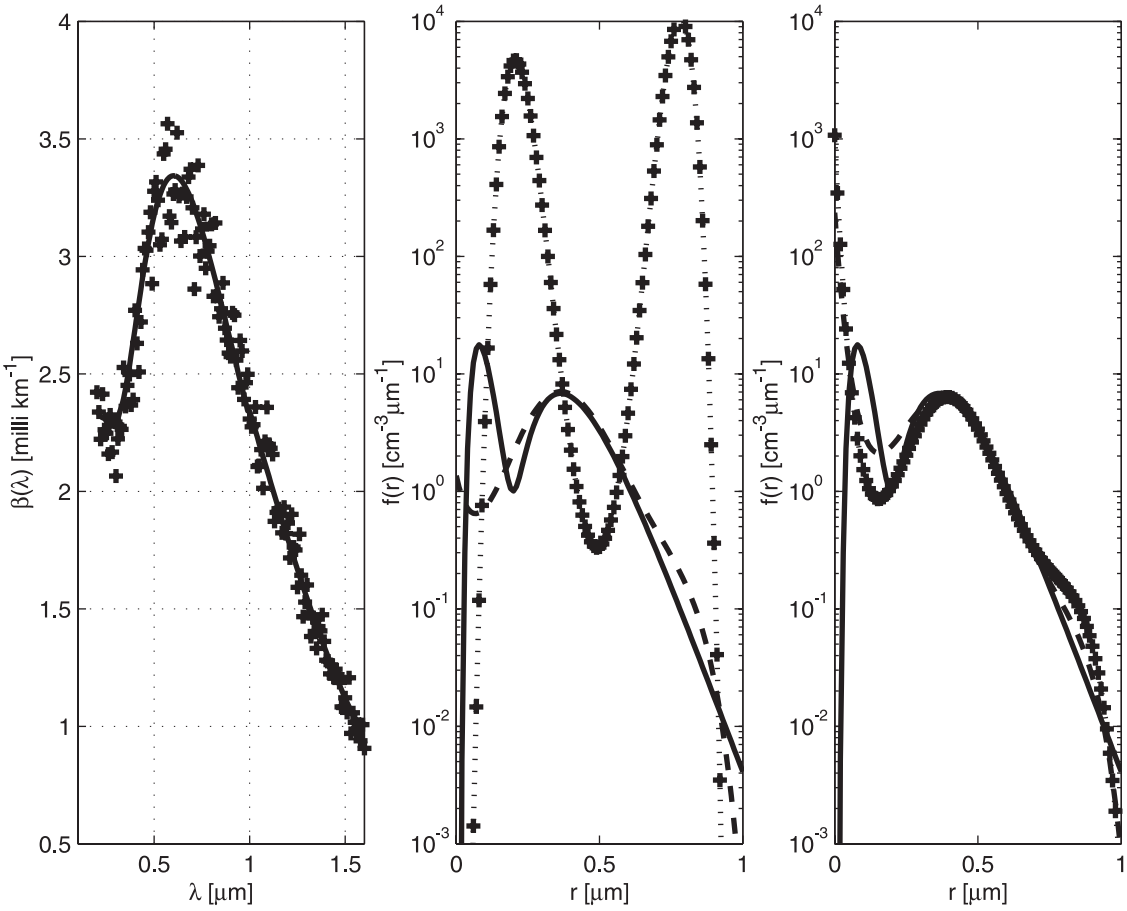

Figure 7. (left) The test case signal F (full line) with 5% Gaussian noise added (crosses). (middle) Exact F distribution (full line); least squares solution ($\theta_i = 0$ in equation (15)) without added noise (dashed line); the same least squares solution with added noise (dotted line with crosses). (right) Same as for central subplot but by using the SIM3 method.

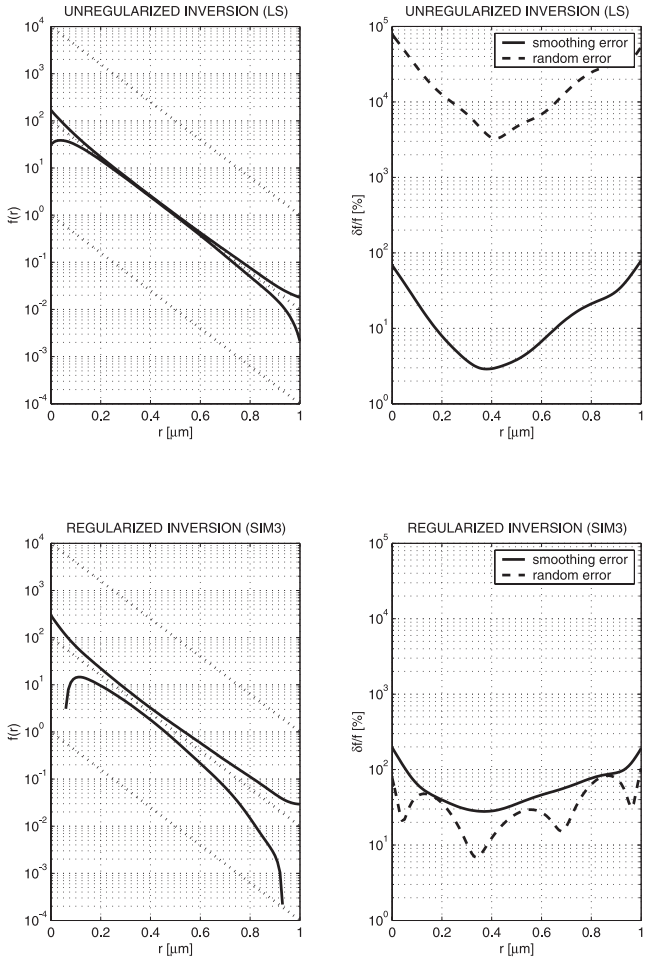

Figure 8. Unregularized inversion of the median extinction coefficient (full line); dotted lines refer to the limits and median of possible solutions. Lower panels are the same for the SIM3 solution. The top right panel shows relative random and smoothing errors for the least squares solution. The lower right panel is the same for the SIM3 solution.

value of the expected random error level. Finally, as a synthetic method similar to table look-up procedures, SIM requires the main computational cost to be incurred in the simulation phase whereas the operational use of the inversion formula is almost instantaneous, a nonnegligible advantage over iterative nonlinear inversion schemes.

[27] **Acknowledgments.** This work was partly performed within projects "SADE (Prodex 6)," "Measurement, understanding and climatology of stratospheric aerosols" (grant MO/35/004), and "Atmospheric microphysics between tropopause and mesopause" (grant MO/35/009) funded by the SSTC/DWTC service of the Belgian Government.

References

Dubovik, O., and M. D. King, A flexible inversion algorithm for retrieval of aerosol optical properties from Sun and sky radiance measurements, *J. Geophys. Res.*, *105*, 20,673–20,696, 2000.

Fussen, D., F. Vanhellemont, and C. Bingen, Optimal spectral inversion of atmospheric radiometric measurements in the near-UV to near-IR range: A case study, *Opt. Express*, *10*, 70–82, 2002a.

Fussen, D., F. Vanhellemont, and C. Bingen, Synthesis inverse mapping: A robust method applicable to atmospheric remote sounding, *J. Geophys. Res.*, *107*(D20), 4421, doi:10.1029/2002JD002206, 2002b.

Golub, G. H., and C. F. Van Loan, *Matrix Computations*, Johns Hopkins Univ. Press, Baltimore, Md., 1996.

King, M. D., D. M. Byrne, B. M. Herman, and J. A. Reagan, Aerosol size distributions obtained by inversion of spectral optical depth measurements, *J. Atmos. Sci.*, *35*, 2153–2167, 1978.

Rodgers, C. D., *Inverse Methods for Atmospheric Sounding*, World Sci., River Edge, N.J., 2000.

Schmid, B., C. Matzler, A. Heimo, and N. Kampfer, Retrieval of optical depth and particle size distribution of tropospheric and stratospheric aerosols by means of Sun photometry, *IEEE Trans. Geosci. Remote Sens.*, *35*, 172–181, 1997.

Steele, H. M., and R. P. Turco, Retrieval of aerosol size distributions from satellite extinction spectra using constrained linear inversion, *J. Geophys. Res.*, *102*, 16,737–16,747, 1997.

Thomason, L. W., A diagnostic stratospheric aerosol size distribution inferred from SAGE II measurements, *J. Geophys. Res.*, *96*, 22501–22508, 1991.

Twomey, S., *Introduction to the Mathematics of Inversion in Remote Sensing and Indirect Measurements*, Elsevier Sci., New York, 1985.

Yue, G. K., A new approach to retrieval of aerosol size distributions and integral properties from SAGE II aerosol spectra, *J. Geophys. Res.*, *104*, 27491–27506, 1999.

C. Bingen, D. Fussen, and F. Vanhellemont, Institut d'Aéronomie Spatiale de Belgique, 3, avenue Circulaire B-1180 Brussels, Belgium. (christb@oma.be; didier@oma.be; filipv@oma.be)